Quantifying the optical properties of turbid media using polarization sensitive hyperspectral imaging (SkinSpect): two-layer optical phantom studies

Fartash Vasefi [a], Nicholas MacKinnon [a], Rolf Saager [b], Anthony J. Durkin [b], Robert Chave [a], Daniel L. Farkas [a, c,*]

[a] Spectral Molecular Imaging Inc., 201 N. Robertson Blvd, Beverly Hills, CA, USA
[b] Beckman Laser Institute and Medical Clinic, University of California, Irvine, CA
[c] Department of Biomedical Engineering, University of Southern California, Los Angeles, CA, USA

ABSTRACT

A polarization-sensitive hyperspectral imaging system (SkinSpect) has been built and evaluated using two-layer tissue phantoms, fabricated to mimic the optical properties of melanin in different epidermal thickness and hemoglobin in dermal layers. Multiple tissue-mimicking phantoms with varying top layer thicknesses were measured for optical system calibration and performance testing. Phantom properties were characterized and validated using SkinSpect. The resulting analysis shows that the proposed system is capable of distinguishing and differentiating the layer-dependent absorption spectra and the depths at which this absorption occurs.

Keywords: hyperspectral imaging, tissue-mimicking phantoms, dermoscope, multimode optical imaging, skin, spectroscopy, optical biopsy, diffuse reflectance, melanoma, polarization imaging.

1. INTRODUCTION

Proper staging of melanoma is vital for defining prognosis and for determining the optimum treatment method. Breslow's depth has been used since the 1970's [1] in staging melanoma progression that defines how deeply tumor cells have invaded. For stage I melanoma, the maximal depth is up to 0.76 mm while for stage V melanoma the depth is greater than 3 mm. Measurement of Breslow's depth is clinically significant and correlates to the five-year survival rate[1]. Survival rates strongly favor early diagnosis, ranging from 98.2% for early, primary site detection to 15.1% for late or metastasized detection, according to a recent 5-year study [3]. Approximately $2.4 billion is spent in the United States each year on melanoma treatment [4]. Clinical costs per case average $4,648 for early and $159,808 for late detection. Diagnosing melanoma earlier can produce significant cost-savings [5].

A dermatologist's visual examination is the standard method for melanoma diagnosis [6]-[10], during which the practitioner looks for abnormalities in mole shape, size and color. Around 2 million biopsies are performed annually to detect melanoma, and the vast majority of these (well over 80%) are benign [11]. Histopathologic examination from skin biopsy is still the gold standard in confirming melanoma [12]. Full-thickness excisional biopsy of lesions is recommended (margin of 1 mm to 2 mm) to provide complete histopathologic assessment and accurate staging of the tumor [13].

Recently, more complex imaging/sensing systems that quantify anatomical and physiological information about skin constituents such as SIAscope IV [14] have been developed. Instrumentation employing intracutaneous analysis with SIAscopy is designed to provide mapping of skin chromophores (melanin, hemoglobin, and collagen). It was reported to have high sensitivity of 96.2 % but the specificity was low at 56.8% [14]. A recent independent study published in 2013 [15] concluded that: (i) SIAscopy-based results have low diagnostic accuracy for melanoma, (ii) single SIAscopic features do not provide reliable diagnostic information relating to the lesions' internal structure on histopathology examination and (iii) SIAscopy cannot be used as a guide for localizing the maximum lesion thickness (for histopathological examination).

*dlfarkas@gmail.com; phone 1 310 858 1670; www.opmol.com

Imaging, Manipulation, and Analysis of Biomolecules, Cells, and Tissues XIII, edited by Daniel L. Farkas, Dan V. Nicolau, Robert C. Leif, Proc. of SPIE Vol. 9328, 93280A · © 2015 SPIE
CCC code: 1605-7422/15/$18 · doi: 10.1117/12.2186031

Tissue quantification results from single-mode optical systems (i.e. individual fluorescence, multispectral, or polarization imaging) have shown that it is very difficult to characterize tissue properties with adequate sensitivity and specificity since most of the skin tissue components' optical properties overlap with each other (i.e. melanin absorption and collagen fluorescence [16], and melanin and hemoglobin absorptions [17]-[19]). In our approach, we use a model-based method to quantify biologically and physiologically plausible tissue characteristics (i.e. melanin, hemoglobin distribution, etc.) from our measurements. Our primary goal is to accurately measure the intracutaneous distribution of melanocytes. We need to distinguish the hemoglobin absorption from the melanin absorption to provide an accurate measurement of this distribution. We have recently shown that SkinSpect multimode measurements can correct mis-estimations (e.g. melanin-hemoglobin mis-estimation described in [18],[19]), and/or cross-talk specific to any individual mode. Figure 1 shows the photon penetration at different wavelengths. Photons have absorption properties proportional to their energy level and hence less diagnostic probing depth in the blue and green wavelength range compared to red and near-infrared wavelength range.

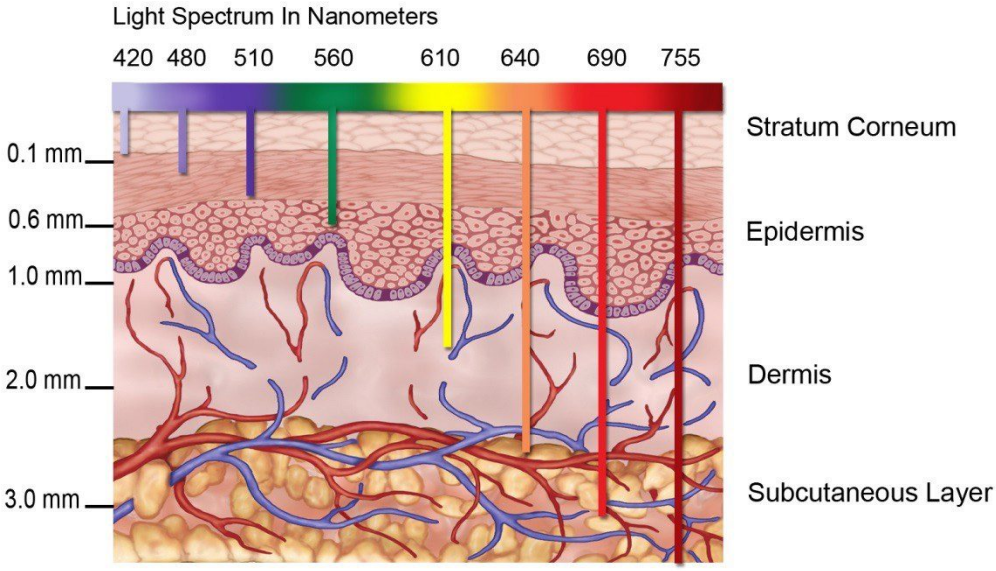

Figure 1 Optical penetration of visible spectrum in skin.

To determine the performance of our polarization-sensitive hyperspectral imaging system for depth assessment, we fabricated and analyzed multiple two-layer tissue-mimicking phantoms with various top layer thicknesses. Correlation between SkinSpect measurements and top layer depth can provide more insight on the potential of SkinSpect for non-invasively staging melanoma. The effect of top layer thickness to the attenuation spectra in perpendicular polarization state has been shown. The importance of hemoglobin quantification before characterizing melanin thickness was discussed. This melanin and hemoglobin characterization overlap will signify the importance of using multimode dermoscope for complete skin analysis.

2. MATERIALS AND METHODS

SkinSpect system

The SkinSpect imaging system combines fluorescence, polarization control and hyperspectral imaging technologies with 30 - 50 wavelength bands available in visible and near infrared wavelength ranges. Our original hand-piece in the research prototype (Figure 2) device employed two cameras, two polarizers, and a pellicle beam-splitter that enables the capture of images in both parallel and cross polarization states (more details in [19]). These two states are required to get the advantages of polarization-based imaging discussed above, such as the removal of specular reflection, enhancement of signals from the lower layers, and discerning the depth of a suspected melanoma. A hyperspectral imaging system

(SkinSpect) illuminates the phantom with spectrally-programmable linearly-polarized light at 33 wavelengths between 468nm and 857 nm. Diffusely reflected photons are separated into collinear and cross-polarized image paths and images captured for each illumination wavelength. We have developed a method which combines two depth sensitive techniques: polarization, and hyperspectral imaging, to accurately determine the spatial distribution of melanin and hemoglobin oxygenation in a skin lesion.

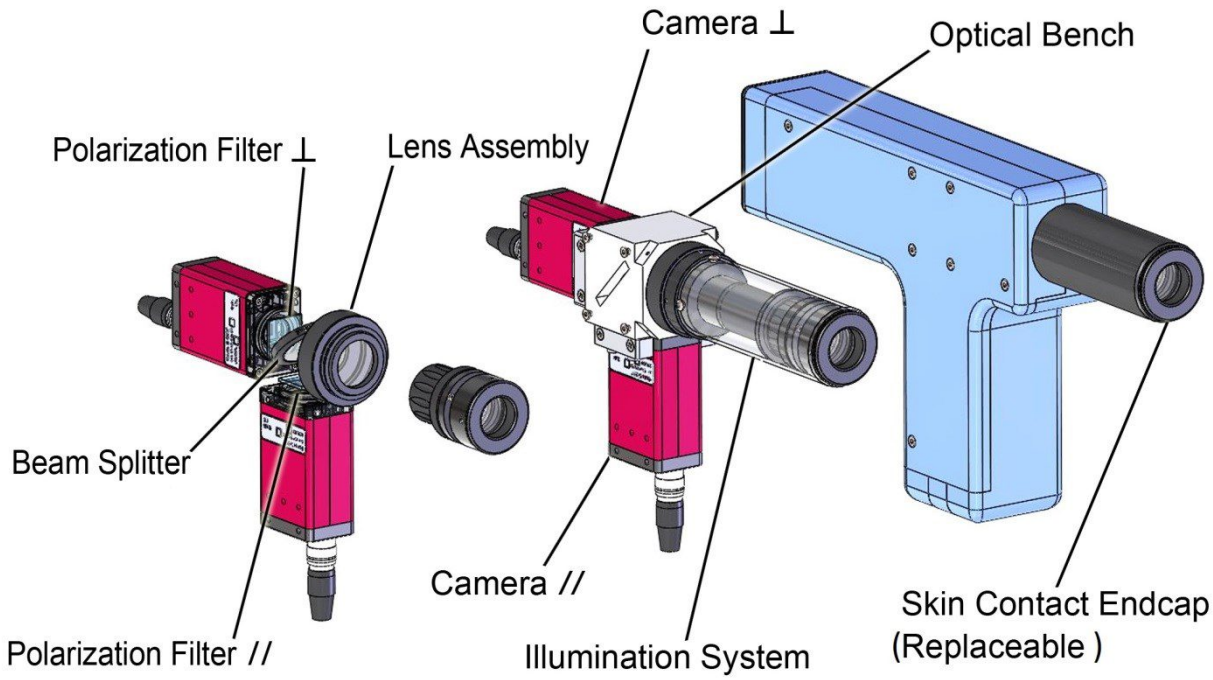

Figure 2. SkinSpect dual-camera hand-piece prototype design.

Two-layer optical phantoms

The tissue simulating skin phantoms used in this study are designed as a two layer model. Interchangeable layers of polydimethylsiloxane-based (PDMS) phantoms are used to simulate dermal and epidermal tissue and evaluate the efficacy and accuracy of this depth-sensitive method. These phantoms used 1) coffee to approximate epidermal melanin absorption in the top layer and 2) bovine hemoglobin in the (semi-infinite) base layer to approximate dermal absorption. Titanium dioxide was used as a scattering agent in all phantom layers. In these tests, five different top layer were used; each of the same optical properties (i.e. absorption and scattering coefficients), but vary in a uniform thickness between 120 and 550 microns.. These five top-layers are assembled in combination with two thick base layers (~3 cm thickness), representing the dermis. Here, the base layer was prepared in with two different concentrations of bovine hemoglobin, mimicking typical and elevated hemoglobin (Hb) levels in the skin. Combinations of five top layers with two base layers yield an array of ten different test configurations. The five variations in thickness on the upper layer with constant optical properties, and the two variations in optical properties on the substrate, permit an isolated confirmation of the model's ability to infer depth of the upper layer. Table 1 summarizes the optical properties, thickness, and the materials used in phantom fabrication process. More details on phantom fabrications are described in [20].

Table 1. Targeted optical properties of two-layer phantoms.

	Top layer	**Base layer #1 (typical)**	**Base layer #2 (elevated)**
Absorption at 650 nm	0.2 mm^{-1}	0.03 mm^{-1}	0.05 mm^{-1}
Scattering at 650 nm	2.0 mm^{-1}	1 mm^{-1}	1 mm^{-1}
Thickness	120 μm, 240 μm, 330 μm, 430 μm, 550 μm	3 cm	3 cm
Materials	Coffee (10 mg/mL) TiO_2 (2 mg/mL)	Dried Bovine Hb (0.05 mg/mL) TiO_2 (1.05 mg/mL)	Dried Bovine Hb (0.1 mg/mL) TiO_2 (1.05 mg/mL)

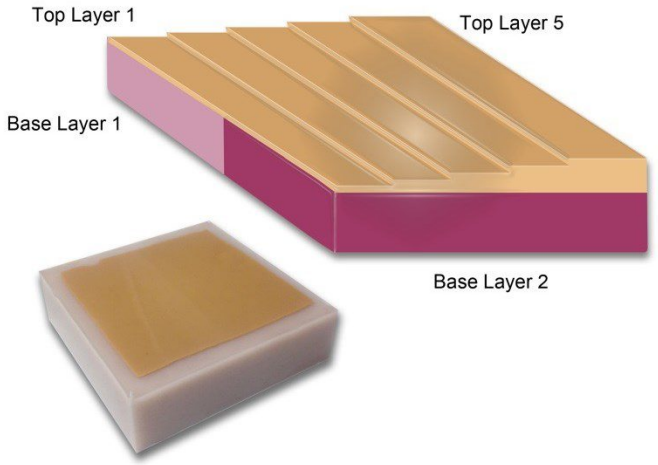

Figure 3. Two-layer phantom structure with five top layer thicknesses and two base-layer concentrations.

The light returned from the phantom is filtered for parallel and perpendicular polarizations. The difference between spectral attenuation between parallel and perpendicular polarization detection is large due to the existence of specular reflection. For parallel polarized incident illumination, there are three components of significance in the flux returned from the incident beam. The first of these is a parallel reflected beam from the first surface which retains its parallel polarization (i.e. specular reflection). The second largest component is the diffuse reflectance from the top layer of the phantom, which is mildly attenuated by the absorbance of the coffee. The third and smallest component of the return flux is the diffuse reflectance from the base layer, attenuated by the bovine hemoglobin and further attenuated by two passes through the top layer of the phantom which can be varied at different layer thicknesses.

3. RESULTS AND DISCUSSION

Figures 4(a) and (b) show the absorption and reduced scattering spectra from the top (epidermal) layer of the phantom. The optical properties of each phantom are calculated by the Inverse Adding-Doubling (IAD) method. IAD is well suited for quantification of thin turbid media [21]. Figures 4(c) and (d) show the absorption and reduced scattering spectra from the base (dermal) layer of the phantom. The optical properties of the two base layer phantoms show that the phantom with elevated hemoglobin (red curve) has about a 50% greater absorption coefficient in the 500 nm – 600 nm wavelength range compared to the base layer with a typical hemoglobin concentration (blue curve).

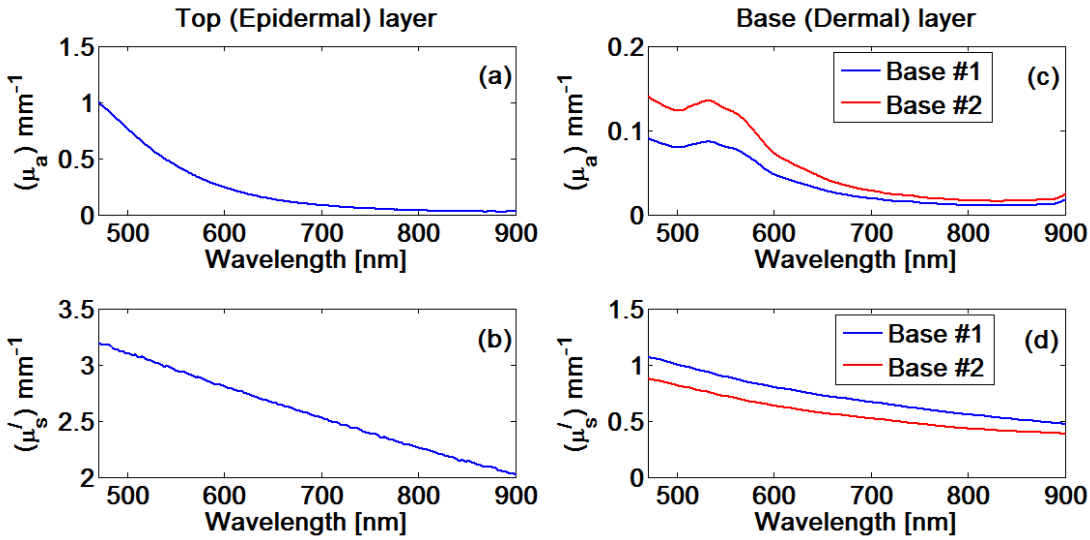

Figure 4. Optical properties of two-layer phantom: (a) absorption and (b) reduced scattering spectra in the top layer, (c) absorption and (d) reduced scattering spectra in the base layer.

The reduced scattering coefficients in the two base-layer phantoms are very comparable. It can be seen in Figure 4 that there is much higher photon absorption and scattering in the top layer compared to the base layer for wavelengths shorter than 550 nm.

In Figure 5 we first compare parallel and perpendicular polarization measurements for a series of phantoms using the first base layer (typical Hb concentration) in combination with five top layers of varying thickness. We then compare the effect of base layer Hb concentration change on the perpendicular polarization measurements with the same set of top layers.

The thickness of the top layer varies from 120±20 μm to 550 ±20 μm (measured by caliper). Figure 5(a) and Figure 5(b) show the attenuation spectra of the same spatial area for both parallel (AcubeP) and perpendicular (AcubeX) polarization measurements, respectively. The attenuation cubes (Acube) calculated from the negative logarithm of calibrated reflectance image stacks in their corresponding polarization states. The AcubeX attenuation is slightly higher than AcubeP due to rejection of the specular reflection from the phantom surface. The AcubeX measurements therefore better represent the top layer thickness structure and optical properties of the two-layer phantoms, independent of surface reflection.

Figures 5(b) and 5(c) compare the attenuation spectra in perpendicular polarization mode between the two base layer concentrations in combination with different thickness top layers. It has been previously shown that melanin has a steady linear decrease trend for absorption in the spectral range from 600-700 nm [24]. The slope of this curve increases proportional to the melanin content of an individual's skin. As shown in Figure 5(b), and 5(c), we notice that the slope of the attenuation spectra is relatively constant for all the two-layer phantoms, especially for the top layer thicknesses between 240 μm and 550 μm.

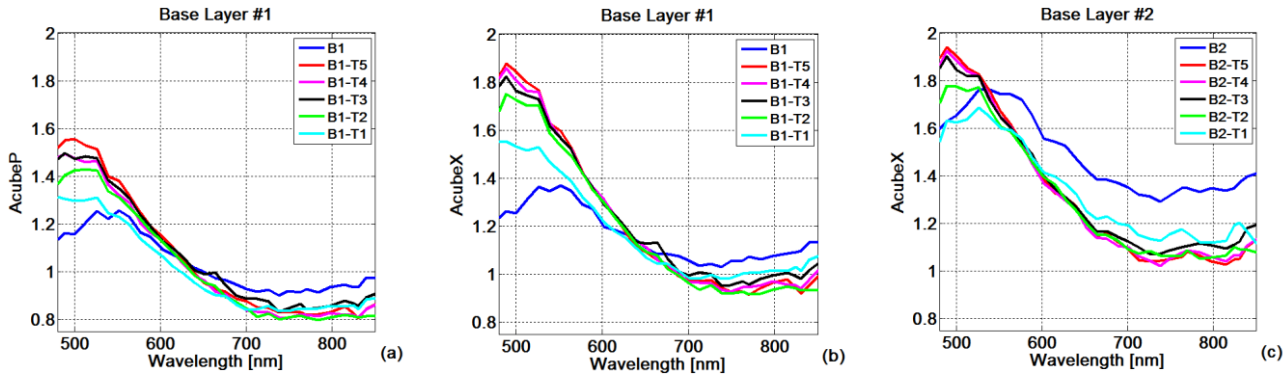

Figure 5. SkinSpect spectral measurements: (a) attenuation spectra of parallel polarization cube of base 1 with top layer 5 thicknesses. (b) Attenuation spectra of perpendicular polarization cube of base 1 with top layer 5 thicknesses. (c) Attenuation spectra of perpendicular polarization cube of base 2 (elevated Hb) with top layer 5 thicknesses.

Figure 6(a) shows the optical penetration depth in the top layer based on the measured optical properties presented in Figure 4. The optical penetration depth is defined as the thickness that causes light to attenuate to 37% its initial value [23] and can be calculated using the following formula.

$$\delta = \frac{1}{\sqrt{3\mu_a\mu_s'}}$$

It is clear that the penetration depth at the 600 nm to 700 nm wavelength range is greater than the top layer thicknesses therefore the photons certainly interact with both the top and base layers. However as shown in Figure 6(b), the AcubeX attenuation slope at the wavelength range of 600 nm to 700 nm has shown a correlation with top layer coffee concentration mostly independent of its thickness.

Another observation from the AcubeX spectra in Figure 4(b) and 4(c) is that the attenuation slope between 489 nm and 513 nm correlates with top layer thickness. As shown in the penetration depth calculation, most of the measured photons within this wavelength range have been scattered from the upper phantom layer and affected by absorption in that layer. Considering that the absorption of the top layer is greater than the base layer at wavelengths shorter than 550 nm, we would expect to have more attenuation in phantoms with a thicker top layer.

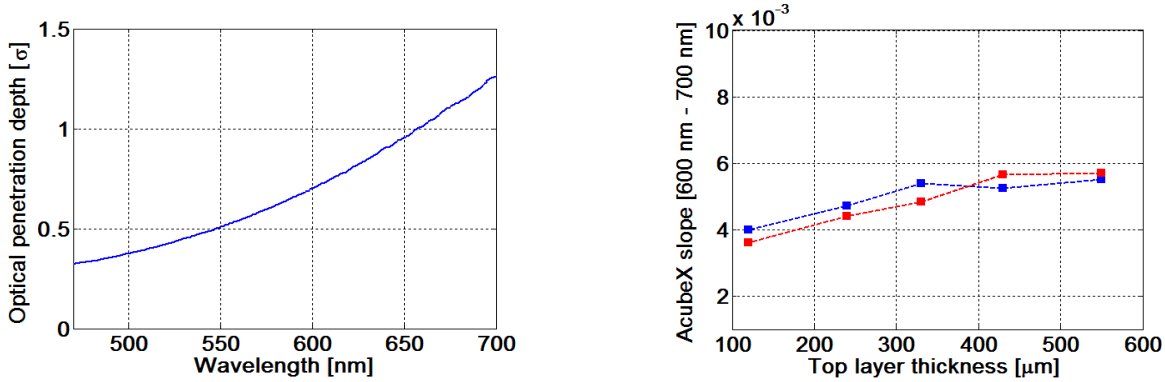

Figure 6. (a) The optical penetration depth in mm top layer. (b) Relative melanin concentrations calculated from AcubX spectra slope at wavelength range of 600 nm to 700 nm (average of 50 by 50 pixels).

Figure 7 shows the AcubeX attenuation slope in the wavelength range between 489 nm and 513 nm versus the top layer thickness. The error bars show the mean and standard variation of the slope for 2600 pixels from the image cubes for each thickness. The correlation between the top layer depth and the AcubeX slope between 489 nm and 513 nm

wavelength range is illustrated. The main difference in the slope changes between the phantoms with different base layers is due to the base layers' different optical properties. It is therefore critical that the optical properties of Hb in dermal layer be accurately characterized in order to characterize melanin depth and concentration.

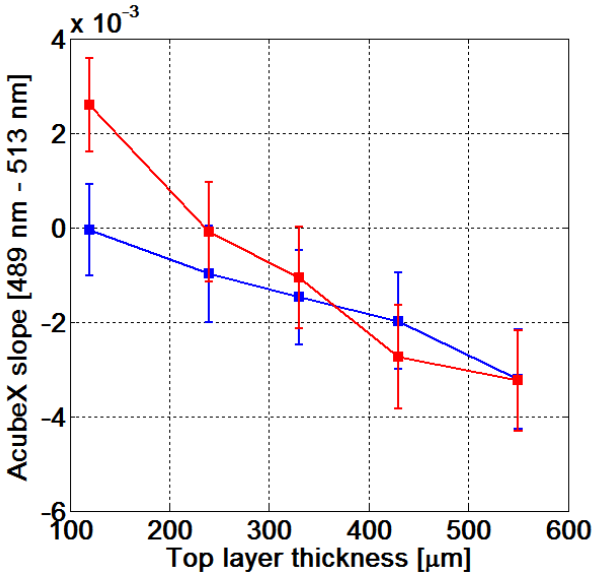

Figure 7. AcubeX spectra slope at wavelength range of 489 nm to 513 nm versus top layer thickness (n = 2600).

4. CONCLUSION

We have built and used a polarization sensitive hyperspectral imager for tissue imaging. The acquired reflection spectra using tissue-mimicking phantoms and their analyses suggest that the system is useful for extracting and quantifying relative chromophore concentrations from different layers in tissues at different depths. We view this as an important step in molecular imaging of skin [18], with implications for early detection of melanoma and non-melanoma skin cancers.

5. ACKNOWLEDGEMENTS

Spectral Molecular Imaging, Inc. (D.L. Farkas, PI) acknowledges support from the US Department of Health and Human Services (under the Qualifying Therapeutic Discovery Program of the Patent Protection and Affordable Care Act of 2010), and by the National Institutes of Health (under -NCI SBIR Grant # 1R44CA183169-01A1). We thank Patricia Vetter for the artwork on Figures 1, 2 and 3.

REFERENCES

[1] Breslow, Alexander. "Thickness, cross-sectional areas and depth of invasion in the prognosis of cutaneous melanoma." Annals of surgery 172(5), 902-908 (1970).
[2] Rubin, Krista M. "Melanoma staging: a review of the revised American Joint Committee on Cancer guidelines." Journal of the Dermatology Nurses' Association 2(6), 254-259 (2010).
[3] SEER Stat Fact Sheets: Melanoma of the Skin. http://seer.cancer.gov/
[4] Costs of Cancer Care report from NCI, Cancer Trends Progress Report – 2011/2012 Update. National Cancer Institute. http://progressreport.cancer.gov/
[5] Alexandrescu, D., "Melanoma costs: a dynamic model comparing estimated overall costs of various clinical stages," Dermatol Online J 15(11), 1 (2009).
[6] Benelli, C., Roscetti, E., Dal Pozzo, V., Gasparini, G., and Cavicchini, S., "The dermoscopic versus the clinical diagnosis of melanoma," Eur J Dermatol, 9(6), 470-476 (1999).

[7] Du Vivier, A.W., Williams, H.C., Brett, J.V., Higgins, E.M., "How do malignant melanomas present and does this correlate with the seven-point checklist? ," Clin Exp Dermatol 16(5), 344–347 (1991).
[8] Higgins E. M., Hall, P., Todd, P., Murthi, R., Du Vivier, A.W., "The application of the seven-point check-list in the assessment of benign pigmented lesions, " Clin Exp Dermatol 17(5), 313-315 (1992).
[9] McGovern, T.W., Litaker, M.S., "Clinical predictors of malignant pigmented lesions. A comparison of the Glasgow seven-point checklist and the American Cancer Society's ABCDs of pigmented lesions, " J Dermatol Surg Oncol 18(1), 22-26 (1992).
[10] Thomas, L, Tranchand, P., Berard, F., Secchi, T., Colin, C., Moulin, G., "Semiological value of ABCDE criteria in the diagnosis of cutaneous pigmented tumors," Dermatology 197(1), 11-17(1998).
[11] Jones, T.P., Boiko, P.E., Piepkorn, M.W., "Skin biopsy indications in primary care practice: a population-based study," J Am Board Farm Pract 9(6), 397-404 (1996).
[12] Goodson, Agnessa Gadeliya, and Douglas Grossman. "Strategies for early melanoma detection: Approaches to the patient with nevi." Journal of the American Academy of Dermatology 60(5), 719-735 (2009).
[13] Tadiparthi, S., S. Panchani, and A. Iqbal. "Biopsy for malignant melanoma–are we following the guidelines?." Annals of the Royal College of Surgeons of England 90, no. 4 (2008): 322.
[14] Moncrieff, M., Cotton, S., Claridge, E., Hall, P., "Spectrophotometric intracutaneous analysis: a new technique for imaging pigmented skin lesions, " Br J Dermatol 146(3), 448-57 (2002).
[15] Terstappen, K., Suurkula, M., Hallberg, H., Ericson, M.B., Wennberg, A.M., "Poor correlation between spectrophotometric intracutaneous analysis and histopathology in melanoma and nonmelanoma lesions, " J Biomed Opt 18(6), 061223-061223 (2013).
[16] Na, Renhua, Ida-Marie Stender, Mette Henriksen, and Hans Christian Wulf. "Autofluorescence of human skin is age-related after correction for skin pigmentation and redness." Journal of investigative dermatology 116, no. 4 (2001): 536-540.
[17] MacKinnon, N., Vasefi, F., Gussakovsky, E., Bearman, G., Chave, R., and Farkas, D.L., "In vivo skin chromophore mapping using a multimode imaging dermoscope (SkinSpect)", Proc. SPIE, 8587, 85870U (2013).
[18] Vasefi, F., MacKinnon, N. B., Farkas, D. L., "Toward in-vivo diagnosis of skin cancer using multimode imaging dermoscopy: (II) molecular mapping of highly pigmented lesions, Proc. SPIE, 8947-18 (2014).
[19] Vasefi, F., MacKinnon, N., Rolf B. Saager, Anthony J. Durkin, Robert Chave, Erik H. Lindsley, and Daniel L. Farkas. "Polarization-Sensitive Hyperspectral Imaging *In Vivo*: A Multimode Dermoscope for Skin Analysis." (Nature) Scientific Reports 4, 4924. 1-10 (2014).
[20] Saager, Rolf B., Clement Kondru, Kendrew Au, Kelly Sry, Frederick Ayers, and Anthony J. Durkin. "Multilayer silicone phantoms for the evaluation of quantitative optical techniques in skin imaging." In BiOS, pp. 756706-756706. International Society for Optics and Photonics (2010).
[21] S. A. Prahl, M. J. C. van Gemert, and A. J. Welch, “Determining the optical properties of turbid media by using the adding-doubling method,” Appl. Optics, 32, 559-568 (1993).
[22] Kollias, N, and Baqer, A., "On the assessment of melanin in human skin in vivo," Photochem Photobiol. 43, 49–54 (1986).
[23] Paulo R. Bargo, Teresa Goodell RN, Rodger Sleven MD, George Kovall MD, Greg Blair MD, Steven L. Jacques, “Optical Measurements for Quality Control During Photodynamic Therapy”, Plenary Talk at Intl. Photodynamic Association meeting, June 7, 2001, Vancouver BC, Canada.
[24] Vasefi, F., MacKinnon, N., and Farkas. D.L. "Toward in vivo diagnosis of skin cancer using multimode imaging dermoscopy: (II) molecular mapping of highly pigmented lesions." In SPIE BiOS, pp. 89470J-89470J. International Society for Optics and Photonics, 2014.